
Free Vibration of the Damping Beam Using Co-simulation Method Based on the MFT

D. Q. Wang, C. J. Wu and R. C. Yang

School of Mechanical Engineering, Xi'an Jiaotong University, Xi'an, Shanxi, China

(Received 6 October 2013; accepted 12 May 2014)

The particle damping technique has been in development for several decades, and has been used successfully in many fields. However, it is difficult to predict its damping characteristics due to complex collisions and friction mechanisms, as well as high non-linear damping characteristics in dense particles. The focus of these current main achievements is centralized on the equivalent single degree of freedom (SDOF) system under free and forced vibration. In this paper, a brand new co-simulation approach for the continuum structure system based on the multiphase flow theory (MFT) of gas solid is developed by the COMSOL Multiphysics live link for MATLAB. A simple continuum structure system, (*i.e.*, the cantilever particle damped beam) is made as an experiment. It is further shown that the damping capacity of a cantilever beam depends not only on the exerted location of the particle damper, but also the quantity of the filling. An experimental verification is performed, and an acceptable accordance is achieved between the theoretical results and the experimental data. It can be shown that the theoretical work in this paper is valid. The co-simulation method simplifies the complicated modelling problem, and offers the possibility to analyse the vibro-acoustic response prediction for complicated particle-damping composite structures.

1. INTRODUCTION

Granular particle damping, which is derived from the impact damping, is a promising technique of providing damping with granular particles placed in an enclosure attached to or embedded in the holes drilled in the vibrating structure.^{1,2} This emerging technology can perform well even in extreme temperatures (either low or high) and harsh chemical environments where traditional passive damping methods, such as the widely used viscous and viscoelastic dampers, are ineffective in particular applications. Particle damping technology has drawn the attention of many researchers in engineering and academic fields, and has been well researched for several decades, with a large volume of books and papers published on the subject. With the development of the particle damping technology in many fields, coherent computer simulation technology is also being developed. The simulation method is very convenient in investigating the effect of the system parameters on the characteristic of the particle damping without extensive trial-and-error testing. However, the popular simulation approaches in the published studies were more often focused on the single degree of freedom (SDOF) system or the equivalent SDOF under the free and forced vibration. It is noted that these current methods have been stretched beyond their normal capacity for the simulation of the continuum damping structure system. Consequently, it is desirable to develop a new simulation technology to predict the characteristics of particle damping. Even to this day, the simulation methods to evaluate the damping characteristic of the continuum structure systems, such as the plate and shell with the particle damper, are rare in recent research. The principal challenges are that their performances are highly nonlinear. There has also been some considerable research in the area of particle damping, and some analytical

models have been developed on heuristic evaluations of particle damping.

The Discrete Element Method (DEM) simulation has been extensively developed over the years to evaluate the dissipative properties of granular materials. The DEM simulation can capture the complex interactions of the dissipation mechanisms in a particle damper. However, the DEM simulation suffers from a complicated dynamic model, and it is highly time-consuming, which make it difficult to perform parametric analysis when the number of granules is large. It is very regrettable that the application field is only limited to the SDOF system, and therefore is not competent for the vibration analysis of the complicated continuity system with particle damper. Saeki³ used this method and investigated the damping behaviour of a horizontally vibrating system in which the gravity is not as important as in a vertically vibrating system. Mao and coworkers⁴ studied the characterization of particle damping in transient vibrations.

Friend *et al.*⁵ developed a lumped mass approach, also referred to as the numerical algorithm, where the particles inside the cavity are assumed to form a lumped mass without consideration of collision and friction effects between particles. The particle damper is attached to the free end of a cantilevered aluminium beam, and the system is reduced to an equivalent SDOF system. The effects of acceleration amplitude and clearance inside the enclosure were studied, and the damping was found to be highly nonlinear, *i.e.*, amplitude dependent. Such an approach is also applicable to investigate the damping performance of the multiple degree-of-freedom (MDOF) system to multi-body vibrating structure.⁶

Liu, *et al.*⁷ used an equivalent viscous damping model to represent the nonlinearity, which was extracted from experimental results. However, their studies were limited to the

use of a single mass to simulate all particles, and the relative motions between the particles were neglected. Papalou and Masri^{8,9} developed a simple model to predict the performance of a particle damper. This model was empirically derived from experiments on a SDOF system.

Our previous work (Wu, *et al.*¹⁰) originally introduced the multiphase flow theory (MFT) of gas solid to evaluate the characteristics of granular particle damping. It is convenient to investigate the performance of particle damping in terms of the effective viscosity. The numerical and experimental studies showed that the particles are helpful to add damping for attenuating the vibration responses of the host structures. Fang and Tang¹¹ further utilized this theory to carry out detailed studies under various forced excitation levels, packing ratios and enclosure dimensions, and the different energy dissipation mechanisms were also quantitatively analysed. Wu, *et al.* further improved the analytical model based our proceeding work,¹⁰ where the expression of equivalent viscous damping for inter-particle friction was introduced instead of the expression of Coulomb friction damping based on the Hertz contact theory discussed in work by Wu, Liao, and Wang.¹⁰ Two typical examples^{12,13} - the free vibration of a cantilever particle-damping beam (equivalent SDOF system) and the harmonic forced vibration of a SDOF system with particle damping were used to verify this improved model.

However, the above research achievements were all limited on the SDOF system. If the continuum structure system is subjected to the particle damper, it is obvious that this analysis can be very complicated. In the real engineering field, the structure can not reasonably be approximated as a SDOF system, since the complex external loading and the damper impacting are likely to excite more than just the fundamental mode of vibration. The primary objective of this paper is to develop a new simulation method with low time-consuming for the complex continuous structure with particle damper based on MFT. In the next section, for the sake of brevity, here a simple particle-damping beam is considered as an attempt.

2. BASIC THEORY

As mentioned by Fan and Zhu,¹⁴ granular particles enclosed in a cavity of a vibrating structure can be considered as a multiphase flow of gas solid with low Reynolds number where the particle concentration is high (*i.e.* the flow is dense). For inelastic particles and a simple shear flow such as a laminar flow, the effective viscosity due to inter-particle collisions can be derived from the kinetic theory of dense multiphase flow as follows:

$$\mu_c = \frac{6}{5}(1 + e_p)\sqrt{\frac{\Theta}{\pi}}\alpha_p^2 g_p \rho_p d_p; \quad (1)$$

where μ_c is the effective viscosity due to inter-particle collisions, e_p is the restitution coefficient of the particle, and α_p is the packing ratio defined as the volume of particles to the total volume of the cavity. ρ_p and d_p denote the density and the mean diameter of particles respectively, Θ is the fluctuation-specific kinetic energy, and g_p is the radial distribution function.

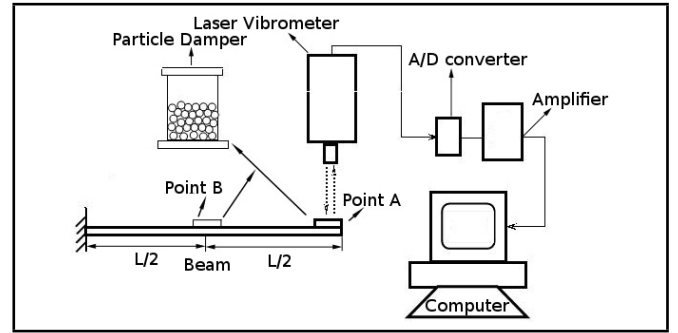


Figure 1. A schematic of a cantilever particle-damping beam and its experimental setup.

Schaeffer¹⁵ conducted a linear analysis of granular flow equations that included frictional stress terms. The equivalent shear viscosity corresponding to friction force between particles can be expressed as follows:¹⁵

$$\mu_f = \frac{p_p \sin \phi}{2\sqrt{I_{2D}}}; \quad (2)$$

where ϕ is the angle of internal friction, I_{2D} is the second invariant of the deviatoric stress tensor. p_p is the solids pressure, which is composed of a kinetic term and a second term due to particle collision.

Considering that the friction model and collision model have the same form of expression, the complete damping effect between the particles can be uniformly expressed as follows:

$$\mu_p = \mu_c + \mu_f. \quad (3)$$

Furthermore, one can find the equivalent viscous damping coefficient due to the inter-particle collisions and friction as shown below (the derivation process of the formulas and the description of parameters can be found in our previous work^{12,13}):

$$c_{eq} = c_1 |\dot{x}|^{1/2} + c_2 |\dot{x}| - c_3 |\dot{x}|^{2/3} + c_4 |\dot{x}| + c_5 |\dot{x}|^2 - c_6 |\dot{x}|^3. \quad (4)$$

Equation (4) shows that the particle damping can be equivalent to the viscous damping, including the inter-particle collisions and friction effects based on the multiphase flow theory (MFT) of gas solid.

As shown in Fig. 1, a granular particle damper is attached to the free end of the beam. The kind of beam can be idealized as a Bernoulli-Euler beam with end mass. Considering the intrinsic structure damping and particle damping, the free vibration equation of the continuous particles damping beam system can be written by the matrix form as

$$\mathbf{M}\ddot{\mathbf{x}} + \mathbf{C}\dot{\mathbf{x}} + \mathbf{K}\mathbf{x} = \mathbf{F} + \mathbf{f}; \quad (5)$$

where \mathbf{M} is the system mass matrix, \mathbf{C} is the system damping matrix, \mathbf{K} is the system stiffness matrix, and \mathbf{F} is the excite force. The viscous damping force $\mathbf{f} = -c_{eq}\dot{\mathbf{x}}$, c_{eq} is derived from the Eq. (4), and $|\dot{x}|$ is the amplitude of vibration velocity on the beam where the particle damper is placed. The Eq. (4) includes the velocity coupling that is found to be highly nonlinear.

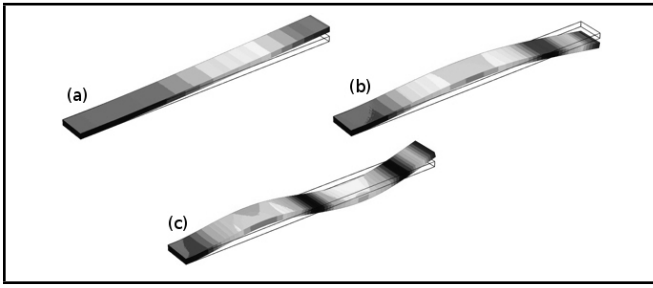


Figure 2. Three first computed bending mode shape of the clamped-free beam: (a) first mode shape, $f_1 = 58.98$ Hz; (b) second mode shape, $f_2 = 369.74$ Hz; (c) third mode shape, $f_3 = 1035.5$ Hz.

It is noted that the effect of the particle damper can be equivalent to a viscous force and a lump mass which includes the mass of the enclosure and the total mass of the particles filled. Such an idea is novel, which leads to a breakthrough that the continuous particle damping structure may be analysed by the commercial software COMSOL Multiphysics live link for MATLAB, using the finite element method (FEM). This step is a key in this article; it becomes an implementation detail process using FEM to analyse a continuous particle damping beam based on MFT of gas solid.

The co-simulation is made by the COMSOL Multiphysics live link for MATLAB by self-programming. Live link provides an interface between COMSOL and MATLAB based on the COMSOL client/server architecture. A COMSOL thin client is running inside MATLAB, and has access to the COMSOL API through the MATLAB Java interface.

On the other hand, the result accuracy of a computer simulation depends on the computational parameters used in the simulation, especially the system parameter Rayleigh damping matrix C . The objective of the next section is to gain the damping parameter C .

3. THE SIMULATION PARAMETERS DETERMINATION

A schematic of the test set-up is shown in Fig. 1. A cantilever beam is chosen as the test specimen to evaluate particle damping performance, in part, because it is an infinite DOF system, as opposed to the SDOF system studied in the literature. The dimensions of the beam are: Young's modulus 66 GPa, density 2828 kg/m³, length 0.38 m, width 0.02 m, and height 0.006 m. To determine the characteristics of the undamped beam, experimental measurements are taken and FEA of the beam is performed using COMSOL. Results from experimental impact testing of the structure indicate that the first three fundamental modes of the structure are 58.99 Hz, 373.27 Hz, and 1041.5 Hz. FEA indicates that this first three fundamental mode are 58.98 Hz, 369.74 Hz and 1035.5 Hz. These values differ slightly from the experimentally determined data, in which the relative errors of FEA values to the experiment values are respectively 0.017%, 0.95%, and 0.58%. The deformed shapes of these modes predicted by the COMSOL are shown in Fig. 2.

In order to quantify the structural damping, it is more appro-

priate to define specific damping capacity as

$$\delta = \frac{\Delta T}{T}; \quad (6)$$

where ΔT is the kinetic energy converted into heat during one cycle of vibration, and T is the maximum kinetic energy during the cycle. If we define a cycle to be the duration between two successive maxima of the structural mass velocity curve $v(t)$, then T is maximum at the start of the cycle and given by

$$T = \frac{1}{2} M V^2. \quad (7)$$

The energy dissipated during the i cycle is calculated as $\Delta T_i = T_i - T_{i+1}$, or

$$\Delta T_i = \frac{1}{2} M (V_i^2 - V_{i+1}^2). \quad (8)$$

Therefore, the energy dissipation of the particle damping is expressed by the specific damping capacity as

$$\delta_i = \frac{V_i^2 - V_{i+1}^2}{V_i^2}. \quad (9)$$

The specific damping capacity applies to linear or nonlinear damping in either transient or steady-state vibrations. In particular, when ξ is small, $\xi \approx \delta/4\pi$ ($\xi < 0.01$). In this study, the value of δ can be found from the experimental data corresponding to the beam without particles (*i.e.* $\alpha_{mp} = 0\%$). At time $t = 0$, the beam is given a tip displacement of $U_0 = 1.5$ mm, released from rest, and allowed to decay freely; the beam vibrates in its fundamental mode. An LK-G3001V Keyence laser vibrometer is used to measure the displacement of the beam. Using the well-known Doppler Effect and the principle of heterodyne interferometry, the displacement is measured by frequency demodulation to an extremely high resolution of 0.1 μm . The displacement amplitude ranges are set from -5 mm to 5 mm. The sampling interval is 250 μs . The value of δ is shown in Table 1. Thus, in the subsequent numerical studies, the value of δ_0 is selected as the mean value for any of four sequenced cycles (*i.e.* $\delta_0 = 0.026477$).

To find the values for the Rayleigh damping, we can use the relationship between the damping ratio and the Rayleigh damping parameters. It is often easier to interpret the critical damping ratios, which are given by

$$\xi = \frac{1}{2} \left(\frac{\alpha_{dM}}{2\pi f} + \beta_{dK} 2\pi f \right); \quad (10)$$

where α_{dM} and β_{dK} are the mass and stiffness damping parameters, respectively; f corresponds to any resonant frequency.

Note that Eq. (10) holds separately for each vibration mode in the system at its resonant frequency. In the frequency domain, it uses frequency-dependent values of α_{dM} and β_{dK} . For example, setting $\alpha_{dM} = 0$ produces an equivalent viscous damping model at the resonant frequency

$$\xi = \beta_{dK} \pi f. \quad (11)$$

Table 1. Specific damping capacity.

Items	1	2	3	4	Mean values
Specific damping capacity	0.023668	0.029749	0.030198	0.022292	0.026477

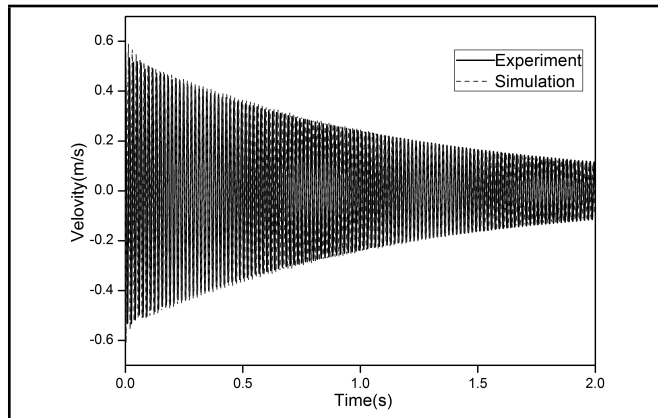


Figure 3. Evolution of the waveforms of velocities in the time domain under free vibration without particles.

Thus,

$$\beta_{dK} = \frac{\xi}{\pi f} = \frac{\delta/4\pi}{\pi f} = \frac{\delta_0}{4\pi^2 f}. \quad (12)$$

Assuming that the structure has a constant damping ratio, the first fundamental mode of the structure is at a frequency of 58.98 Hz. Solving the system of equations above will give the result $\beta_{dK} = 1.14 \times 10^{-5}$.

Figure 3 shows the velocity responses comparison between the simulation by COMSOL and the experimental measurement of the beam without particles. It is noted that the simulation results in COMSOL differ slightly from the experimental results. That is to say, the actual intrinsic structural damping in the experimental is not exactly the Rayleigh damping considered in the COMSOL model.

To verify the theoretical model developed in this study, an experiment for a cantilever beam with a particle damper is set up and shown in Fig. 4. The specifications for the experiment are the same as those specifications used in the simulation for the purpose of comparison. The transient velocity responses are measured. At time $t = 0$, the beam is given an initial tip displacement, released from rest, and allowed to decay freely, and the beam vibrates in its fundamental mode. A laser vibrometer LK-G3001V Keyence is used to measure the velocity responses of the particle damper block.

4. FREE VIBRATION OF A CANTILEVER PARTICLE-DAMPING BEAM

In this section, the transient response of a continuum cantilever particle-damping beam is analysed. The initial value of the tip displacement of the beam is 1.5 mm. The mass of the damper with no particles is 14.52 grams, and its interior dimensions are: diameter = 16 mm, and height = 20 mm. The particle is made of iron powder whose density is 6800 kg/m^3 , and the mean diameter of particles is 0.3 mm. The restitution coefficient of the particles is 0.6 on the basis of testing. The kinetic friction coefficients between the individual particles and between the particles and the wall of the cavity are 0.3 and

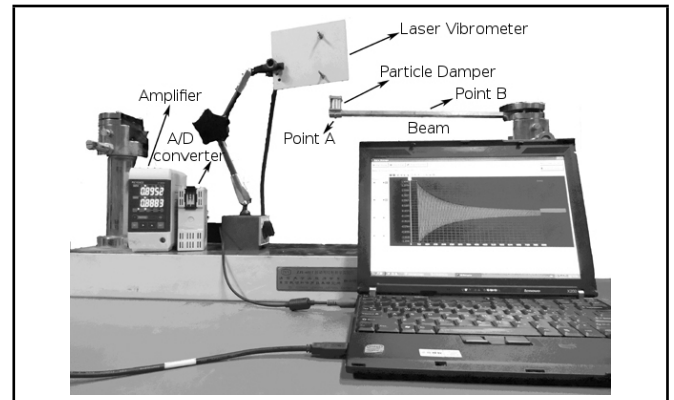


Figure 4. A figure of the experimental apparatus used.

0.2, respectively, from experimental results. In addition, the kinematic viscosity and density of air are $1.51 \times 10^{-5} \text{ m}^2/\text{s}$ and 1.21 kg/m^3 , respectively.

As documented by Wu, Liao, and Wang,¹⁰ the experimental set-up to carry out the free vibrations consists of imposing an initial displacement at the beam tip and allowing it to decay freely. The beam decays freely with known initial displacement and velocity. The mass packing ratio α_{mp} , which is defined as the actual packing mass of particles to the maximum permissive packing mass of particles in a cavity, is also introduced to describe the packing condition of the damper.

The process is organized in two parts. The first part consists of studying the vibratory behaviour of the system under free vibration. The velocity of the whole cantilever beam and enclosure is measured for two cases. In the first case, the mass packing ratio is the same, but the position is different where the particle damper is placed (point A or point B) (Fig. 1). In the second measurement, the mass packing ratio is different, and the particle damper location is the same. In the second part of the process, the fast Fourier transformation of the system velocities obtained in the same experimental conditions are shown for both a system without particles and a system with a particle damper.

To determine the characteristics of the damped system with the particle damper, both experimental testing and FEA are performed. The transient velocity responses are measured. To bring the influence of the mass packing ratio α_{mp} and the location where the particle damper is exerted on the evolution of specific damping capacity, some measurements are performed for the continuous cantilever beam with the enclosure containing the particles.

Figures 5a and 5b show the results of the free vibrations at the free end of the beam when the particle damper is placed in a different position on the beam (see Fig. 1, and the point A or point B), the mass packing ratio is kept for the same values. It is shown that the vibrations of the beam with particles decay much faster when the particle damper is placed on the point A, compared to the case in which the particle damper is placed on the point B.

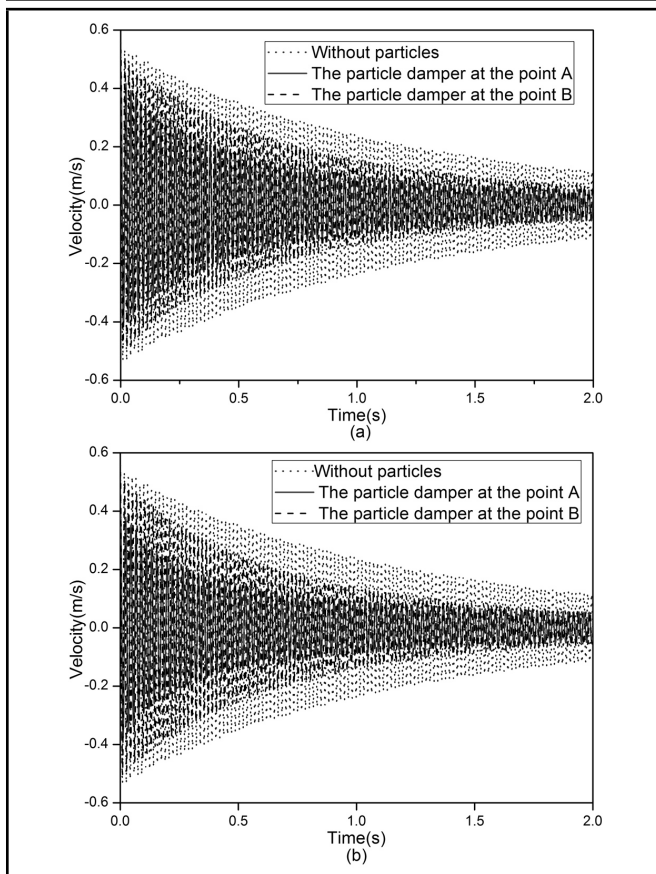


Figure 5. Velocity response at the free end of the beam, when the particle damper is placed on the different position: (a) $\alpha_{mp} = 10\%$; (b) $\alpha_{mp} = 40\%$.

Figures 6a and 6b show velocity response at the free end of the beam, when the particle damper is placed on the same point, the mass packing ratio is kept for the different values. It is shown that the vibrations of the beam with particles decay much faster (with increasing mass packing ratio α_{mp}) compared to the case without particles.

Figures 5 and 6 present a comparison of typical decay curves for the two cases described above. The effects of a particle damper on the velocity amplitude are seen in the differences between the two curves. Clearly, a particle damper causes a significant decrease in the velocities amplitude within the first few cycles.

Figures 7 and 8 show the comparisons of the velocity responses of the beam between the simulation results and the experiments. The simulation results show reasonably accurate estimates of the response of the transient vibration. It is noted that the theoretical results differ slightly from the experimental results. That is to say, the actual intrinsic structural damping in the experiment is not exactly the viscous damping considered in the theoretical model.

In Figs. 9 and 10, the fast Fourier transformation of the system velocities obtained in the same experimental conditions are shown for both a system without the particles and for a system with a particle damper. For the first case, when the particle damper is placed in a different position on the beam, the mass packing ratio α_{mp} is kept for the same values, and the fast Fourier transformation in Figs. 5a and b are corresponding to the experimental data in Figs. 9a and b. For the mass packing

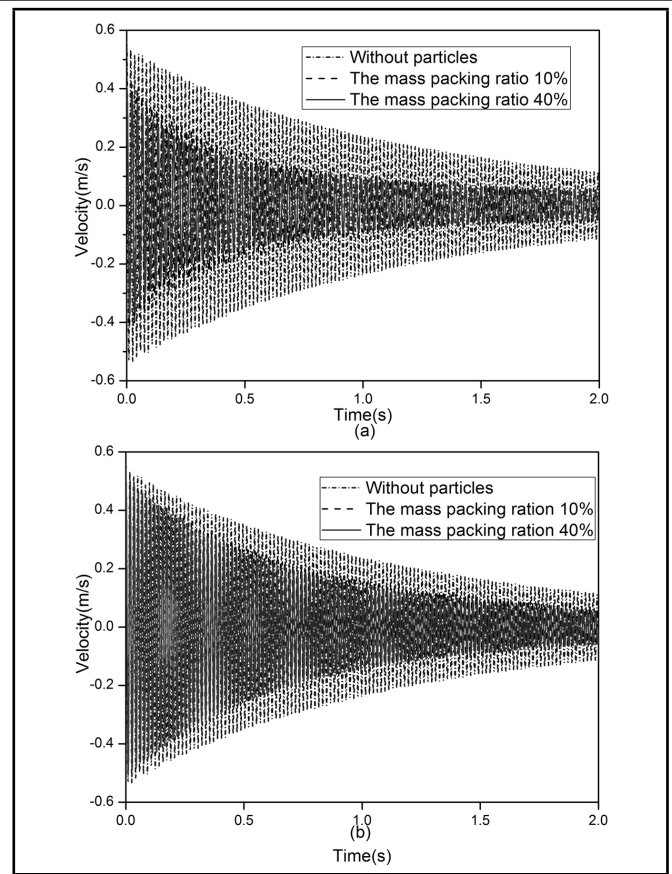


Figure 6. Velocity response at the free end of the beam, when the particle damper is placed on the same position: (a) The particle damper on point A; (b) The particle damper on point B.

ratio $\alpha_{mp} = 10\%$, three spectral peaks could be clearly identified at ≈ 59.5 Hz (without particles), 57.5 Hz (the particle damper on point B) and 46 Hz (the particle damper on point A) in Fig. 5a. The presence of particle collisions reduces the spectral amplitude of these peaks significantly about 12.05% and 33.45% compared to the case without particles, respectively. For the mass packing ratio $\alpha_{mp} = 40\%$, there are three spectral peaks, respectively: z at ≈ 59.5 Hz, (without particles), 56.5 Hz (the particle damper on point B), and 43 Hz (the particle damper on point A) in Fig. 5b. The corresponding spectral amplitude peaks decrease about 30.43% and 58.35% compared to the case without particles.

For the second case, when the particle damper is placed on the same point, but the mass packing ratio is kept for the different values, the fast Fourier transformations of the system velocities in Figs. 6 a and b are correspond to the experimental data in the Figs. 10 a and b. For the particle damper is localized on point B, three spectral peaks appear at ≈ 59.5 Hz (without particles), 57.5 Hz (the mass packing ratio $\alpha_{mp} = 10\%$) and 56.5 Hz (the mass packing ratio $\alpha_{mp} = 40\%$). The corresponding spectral amplitude peaks are lowered about 12.05% and 30.43% compared to the case without particles, respectively. For the particle damper is exerted on point A, three spectral peaks are got at ≈ 59.5 Hz (without particles), 46 Hz (the mass packing ratio $\alpha_{mp} = 10\%$) and 43 Hz (the mass packing ratio $\alpha_{mp} = 40\%$). The peaks of the corresponding spectral amplitude are respectively dropped about 33.45% and 58.35% compared to the case without particles.

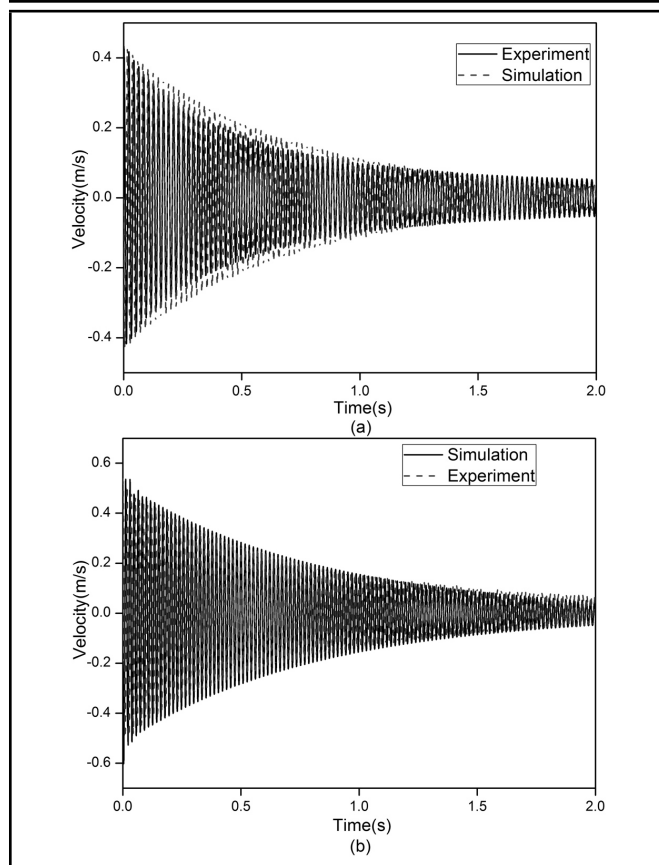


Figure 7. Evolution of the waveforms of velocities in the time domain under free vibration $\alpha_{mp} = 10\%$ (a) the particle damper is placed on point A; (b) the particle damper is placed on point B.

These results prove that total particle mass and the particle damper arrangement appear to have a fairly significant effect on damping for the cantilever beam. Increasing the mass tends to increase damping. And the particle damper which is attached to the structure in a region of high vibration levels can significantly reduce the vibration of the host structures. As might be expected, changes in the total particle mass can lead to a fairly significant shift in the frequency of peak response.

5. CONCLUDING REMARKS

In this article, the specific damping capacity of a cantilever continuous particle damping beam is experimentally studied and simulated. The effect of particle impacts on the vibratory behaviour of the structure is illustrated. A comparison of typical decay velocities in a waveform of the system is conducted without particles and with particles dampers. It is proved that, with a particle damper, a very high value of specific damping capacity can be achieved, compared to intrinsic material damping of the structure. Numerical results show that total particle mass appears to have a fairly significant effect on damping for the cantilever particle damping beam. Increasing the filling mass of the particles tends to increase damping. When the particle damper is exerted on different positions of the beam, the damping properties can present an obvious change. The ideal damping effect can be achieved by putting the particle damper in a position on the structure with high-level vibration.

It is encouraging to note that the novel simulation approach

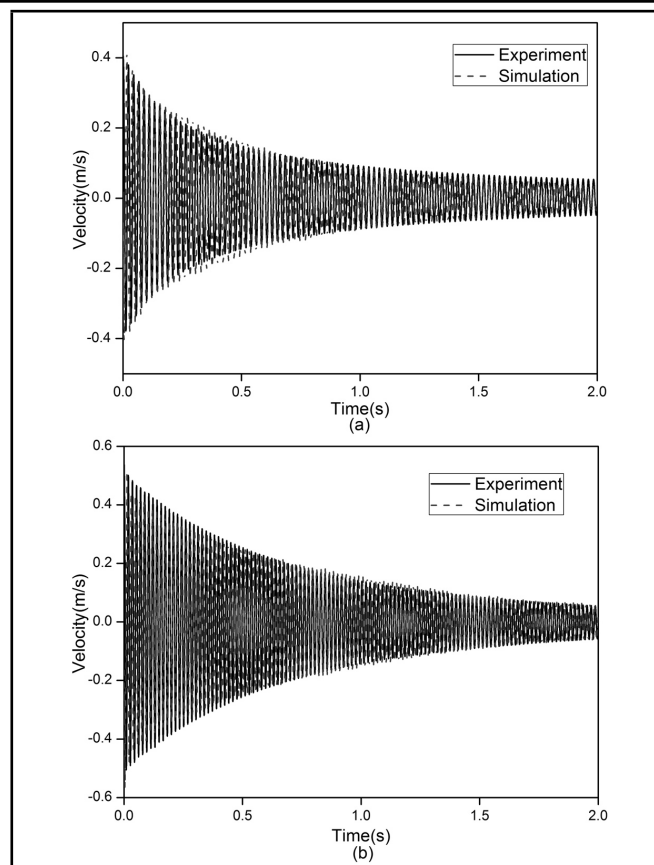


Figure 8. Evolution of the waveforms of velocities in the time domain under free vibration $\alpha_{mp} = 40\%$ (a) the particle damper is placed on point A; (b) the particle damper is placed on point B.

based on MFT of gas solid can accurately and reasonably predict the characteristics of particle damping. The co-simulation of COMSOL Multiphysics with MATLAB will broaden our horizons in the design and application for particle dampers. This method provides an effective instruction to the implementation of particle damping in practice, and offers the possibility to analyse the more complex particle-damping system with lower computational cost than DEM, and it can lay a theoretical foundation for the vibration and acoustic radiation response prediction problem for particle damping composite structures.

ACKNOWLEDGMENTS

The work described in this paper was supported by NSFC (Natural Science Foundation of China) Project No.51075316 and Program for Changjiang Scholars and Innovative Research Team in University (PCSIRT).

REFERENCES

- Chen, T., et al. Dissipation mechanisms of non-obstructive particle damping using discrete element method, *Proc. SPIE 4331, Smart Structures and Materials 2001: Damping and Isolation*, Newport Beach, CA, (2001).
- Fricke, J. R. Lodengraf damping: An advanced vibration damping technology, *SV Sound and Vibration*, **34** (7), 22–27, (2000).

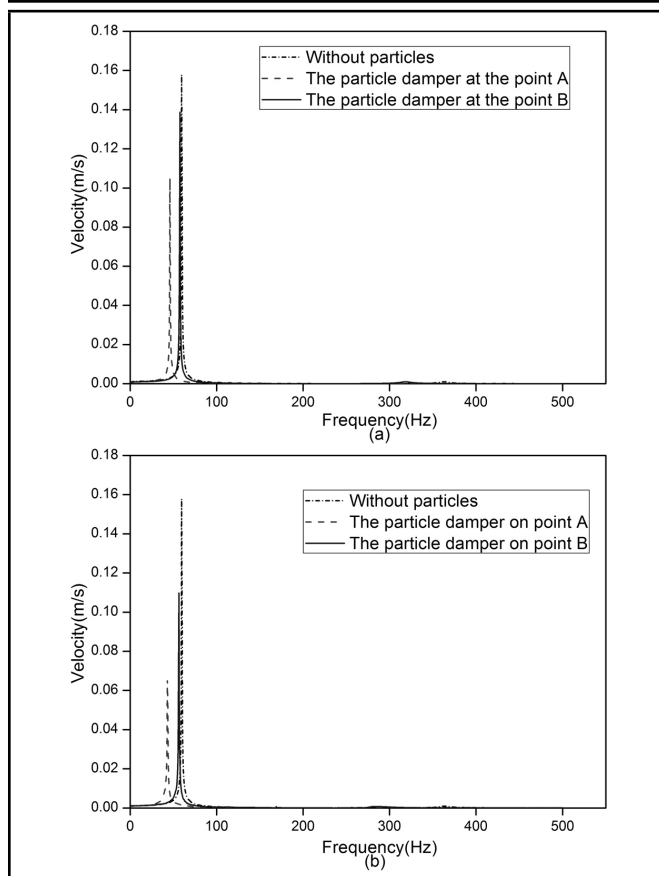


Figure 9. Spectrum of velocities of the system under free vibration, the particle damper is placed on the different position: (a) $\alpha_{mp} = 10\%$; (b) $\alpha_{mp} = 40\%$.

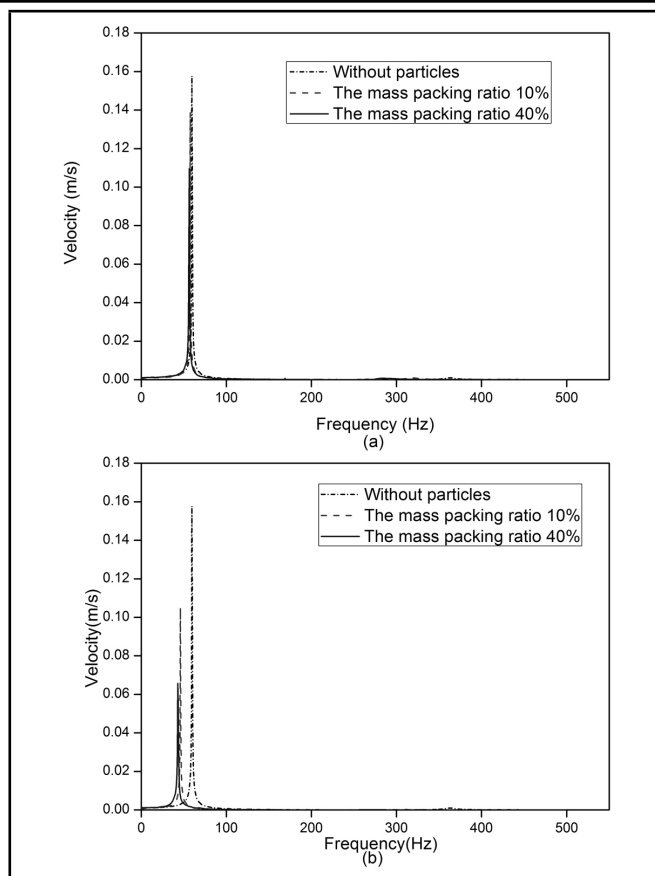


Figure 10. Spectrum of velocities of the system under free vibration, the particle damper is placed on the same position: (a) the particle damper is placed on point B; (b) the particle damper is placed on point A.

- ³ Saeki, M. Analytical study of multi-particle damping, *Journal of Sound and Vibration*, **281** (3), 1133–1144, (2005).
- ⁴ Mao, K., et al. Simulation and characterization of particle damping in transient vibrations, *Journal of Vibration and Acoustics*, **126** (2), 202–211, (2004).
- ⁵ Marhadi, K. S. and Kinra, V. K. Particle impact damping: effect of mass ratio, material, and shape, *Journal of Sound and Vibration*, **283** (1), 433–448, (2005).
- ⁶ Isao, Y., Yoshito, T., and So, N. Y. Particle damping with granular materials for multi-body system, *ICSV 15 International Congress on Sound and Vibration*, Daejeon, Korea, (2008).
- ⁷ Liu, W., Tomlinson, G. R., and Rongong, J. A. The dynamic characterisation of disk geometry particle dampers, *Journal of Sound and Vibration*, **280** (3), 849–861, (2005).
- ⁸ Papalou, A. and Masri, S. F. An experimental investigation of particle dampers under harmonic excitation, *Journal of Vibration and Control*, **4** (4), 361–379, (1998).
- ⁹ Papalou, A. and Masri, S. F. Performance of particle dampers under random excitation, *Journal of Vibration and Acoustics*, **118** (4), 614–621, (1996).
- ¹⁰ Wu, C. J., Liao, W. H., and Wang, M. Y. Modelling of granular particle damping using multiphase flow theory of gas-particle, *Journal of Vibration and Acoustics*, **126** (2), 196–201, (2004).
- ¹¹ Fang, X. and Tang, J. Granular damping in forced vibration: Qualitative and quantitative analyses, *Journal of Vibration and Acoustics—Transactions of the ASME*, **128** (4), 489–500, (2006).
- ¹² Wu, C. J., Yang, R. C., and Wang, D. Q. Prediction on vibration response of a cantilever particle-damping beam based on two-phase flow theory of gas-particle, *Chinese Journal of Mechanical Engineering*, **49** (10), 53–61, (2013).
- ¹³ Wu, C. J., Yang, R. C., and Wang, D. Q. An improved modelling of granular particle damping using multiphase flow theory of gas-particle, *ICSV 20th International Congress on Sound & Vibration*, Bangkok, Thailand, (2013).
- ¹⁴ Fan, L. S. and Zhu, C. *Principles of Gas-Solid Flows*. Cambridge University Press, Cambridge, UK, (1998).
- ¹⁵ Schaeffer, D. G. Instability in the evolution equations describing incompressible granular flow, *Journal of Differential Equations*, **66** (1) 19–50, (1987).